

CORRELATIONS BETWEEN THE SURFACE DENSITY OF DISK GALAXIES AND THE HALO SPIN PARAMETER MEASURED IN HYDRODYNAMIC SIMULATIONS

Ji-HOON KIM¹, JOUNGHUN LEE²

Draft version March 22, 2019

ABSTRACT

Late-type low surface brightness galaxies (LSBs) are faint disk galaxies with central maximum stellar surface densities below $100 M_{\odot} \text{pc}^{-2}$. The currently favored scenario for their origin is that LSBs have formed in fast-rotating halos with large angular momenta. We present the first numerical evidence for this scenario using a suite of self-consistent hydrodynamic simulations of a $2.3 \times 10^{11} M_{\odot}$ galactic halo, in which we investigate the correlations between the disk stellar/gas surface densities and the spin parameter of its host halo. A clear anti-correlation between the surface densities and the halo spin parameter λ is found. That is, as the halo spin parameter increases, the scale radius at which the stellar surface density drops below $0.1 M_{\odot} \text{pc}^{-2}$ monotonically increases, while the average stellar surface density of the disk within that radius decreases. The ratio of the average stellar surface density for the case of $\lambda = 0.03$ to that for the case of $\lambda = 0.14$ reaches more than 15. We demonstrate that the result is robust against variations in the baryon fraction, confirming that the angular momentum of the host halo is an important driver for the formation of LSBs.

Subject headings: galaxies:formation — galaxies:evolution — stars:formation — cosmology:dark matter

1. INTRODUCTION

Still shrouded in mystery are the origin and true nature of dark matter that has long evaded astronomical observations. Astrophysical interest in dark matter has been escalated not only because it is inferred to dominate the matter mass budget of the Universe, but because of the simplicity of its dynamics. In particular, dark matter is thought to not only exist inside galactic-scale halos, but even dominate the galactic gravitational dynamics. Naturally, the records of dark matter dynamics throughout the formation of the galactic halos are imprinted in the morphology of the present-day galaxies. We may therefore advance our understanding of the gravity and the nature of dark matter by investigating the galaxies' structure and formation history. For this purpose, late-type low surface brightness galaxies (LSBs) provide us with a unique and intriguing laboratory.

Late-type LSBs typically refer to the disk galaxies that are fainter than the night sky, exhibiting B -band central surface brightnesses $\mu_{B,0} > 22.7 \text{ mag arcsec}^{-2}$ (Freeman 1970) or equivalently central maximum stellar surface densities $\Sigma_{*,0} < 100 M_{\odot} \text{pc}^{-2}$ (McGaugh et al. 2001). They are different from the under-luminous dwarf spheroidals in that the late-type LSBs may have large disks and high intrinsic luminosities in spite of their low surface brightnesses. Their abundance has long been underestimated, but observations now imply that LSBs may represent a significant fraction of the galaxy population (e.g. Impey & Bothun 1997, and references therein). Since it was realized that a wealth of LSBs inhabit both cluster and field regions, and they may provide an important clue for the galaxy formation process (e.g. Impey et al. 1988; Irwin et al. 1990; McGaugh et al. 1995; Sprayberry et al. 1996, 1997), many studies have explored their physical properties, dynamical states, host halo structures, spatial distribution, and environmental dependences (e.g. McGaugh & Bothun 1994; Mo et al. 1994; Zwaan et al. 1995; de Blok et al. 1996; Mihos et al.

1996; Gerritsen & de Blok 1999; Bell et al. 2000; Matthews & Wood 2001; Bergmann et al. 2003; Kuzio de Naray et al. 2004; Matthews et al. 2005; Boissier et al. 2008; Rosenbaum et al. 2009; Gao et al. 2010; Galaz et al. 2011; Morelli et al. 2012; Zhong et al. 2012; Ceccarelli et al. 2012).

While the origin of LSBs is yet to be fully understood, theoretical modelings to comprehend how LSBs have formed paralleled the above phenomenological efforts. The simplest, but currently favored scenario states that the difference of LSBs from the high surface brightness galaxies (HSBs) results from the fast-spinning motion of their host halos (see §2; Dalcanton et al. 1997; Jimenez et al. 1997; Mo et al. 1998). To quantitatively compare the predictions of this theory with the observed properties of LSBs, Jimenez et al. (1998) utilized simplified models for the physical, chemical, and spectrophotometric evolution of disk galaxies, and found that the theory nicely reproduces the observed properties of LSBs. Their results were later confirmed by Boissier et al. (2003) who used larger and higher quality LSB samples (see §2).

Because LSBs are more dark matter dominant than HSBs (e.g. de Blok & McGaugh 1997; Pickering et al. 1997; McGaugh et al. 2001), LSBs have also been employed to test the nature of dark matter and gravity. Studies have claimed that the rotation curves of LSBs could be useful in constraining the properties of dark matter and even modified Newtonian dynamics (e.g. McGaugh & de Blok 1998a,b; de Blok & McGaugh 1998; Spergel & Steinhardt 2000; Swaters et al. 2010; Kuzio de Naray & Spekkens 2011). Recently Lee et al. (2012) speculated that the abundance of LSBs could be a testbed for modified gravity. Using a high-resolution simulation, they demonstrated that modified gravity may spin up the low mass galactic halos and significantly alter the abundance of LSBs. *Nevertheless*, in order to utilize LSBs as a probe into the nature of dark matter and gravity, it is indispensable to first properly constrain the driver that produces LSBs. Although the galactic evolution models of Jimenez et al. (1998) and Boissier et al. (2003) supported the hypothesis that the LSBs form in the halos with large angular momenta, their results were subject to the simplified prescriptions for the formation of disk galaxies. To improve the situation and advance

¹ Department of Astronomy and Astrophysics, University of California, Santa Cruz, CA 95064, USA; me@jihoonkim.org

² Astronomy Program, Department of Physics and Astronomy, Seoul National University, Seoul 151-747, Korea; jounghun@astro.snu.ac.kr

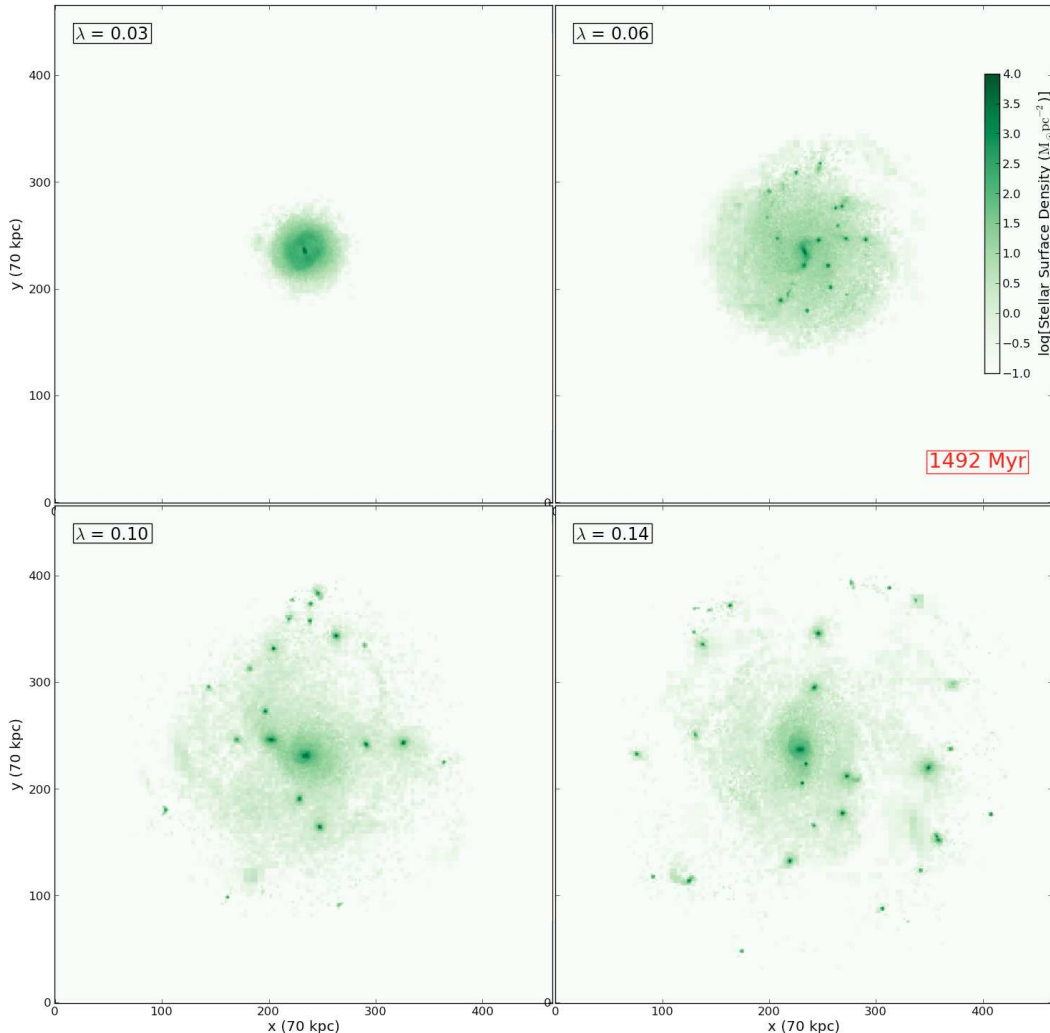


FIG. 1.— Face-on stellar surface densities in a central 70 kpc box at 1.49 Gyrs after the start of the simulation for four different halo spin parameters, $\lambda = 0.03, 0.06, 0.10, 0.14$ in the top-left, top-right, bottom-left, and bottom-right panel, respectively. The initial baryonic mass fraction in the halo is $f_b = 0.10$. Stars of age less than 1 Gyr are used to estimate surface densities. More information on the suite of simulations and analysis is provided in §3 and §4.1.

our understanding of the origin of LSBs, a comprehensive, *self-consistent* hydrodynamic simulation is greatly needed.

In light of this development, we for the first time numerically examine whether or not the angular momentum of the host halo is an important driver for determining the galactic surface brightness. Using a suite of comprehensive hydrodynamic simulations, we quantitatively investigate the correlations between the surface density of a disk galaxy and the spin parameter of its host halo without having to rely on a simplified prescription for galactic evolution. The outline of this article is as follows. We briefly describe the currently popular model for the origin of LSBs in §2, and the set-up of our numerical experiments in §3. The analysis of our simulation results is presented in §4 focusing on the correlation between the stellar/gas surface densities and the halo spin parameter. The robustness of our result is also examined against variations in the initial baryonic mass fraction. Finally we discuss the implications of our results and draw a conclusion in §5.

2. A BRIEF REVIEW OF THE MODEL FOR THE ORIGIN OF LOW SURFACE BRIGHTNESS GALAXIES

A dark matter halo acquires its angular momentum \mathbf{J} through the tidal interactions with the surrounding matter distribution at its proto-halo stage (Peebles 1969; Doroshkevich

1970; White 1984). Since the magnitude of the halo angular momentum is dependent upon its virial mass M_{vir} , it is often convenient to adopt a dimensionless spin parameter $\lambda \equiv |\mathbf{J}|/(2GM_{\text{vir}}R_{\text{vir}})^{1/2}$ with the halo virial radius R_{vir} to quantify how fast a halo rotates around its axis of symmetry. Simulations have shown that the probability density of λ is approximated by a log-normal distribution in Λ CDM cosmology, being relatively insensitive to mass scale, environment, and redshift (e.g. Bullock et al. 2001).

In the gravitationally self-consistent model for the formation of disk galaxies, a rotationally-supported disk forms in a potential well of a dark matter halo through a dissipative gravitational collapse of the baryonic content (Fall & Efstathiou 1980). The resulting baryonic disk shares the same tidally-induced specific angular momentum \mathbf{j} (angular momentum per unit mass) with its host halo. Based on this model, Dalcanton et al. (1997) proposed a scenario that the large specific angular momentum of a dark matter halo disperses the gas to a wider extent, leading to a large disk size and thus a low gas surface density (see also Jimenez et al. 1997; Mo et al. 1998). To relate the gas surface density to the *stellar* surface density and to perform a systematic test of this scenario against observations, Jimenez et al. (1998) computed various galactic

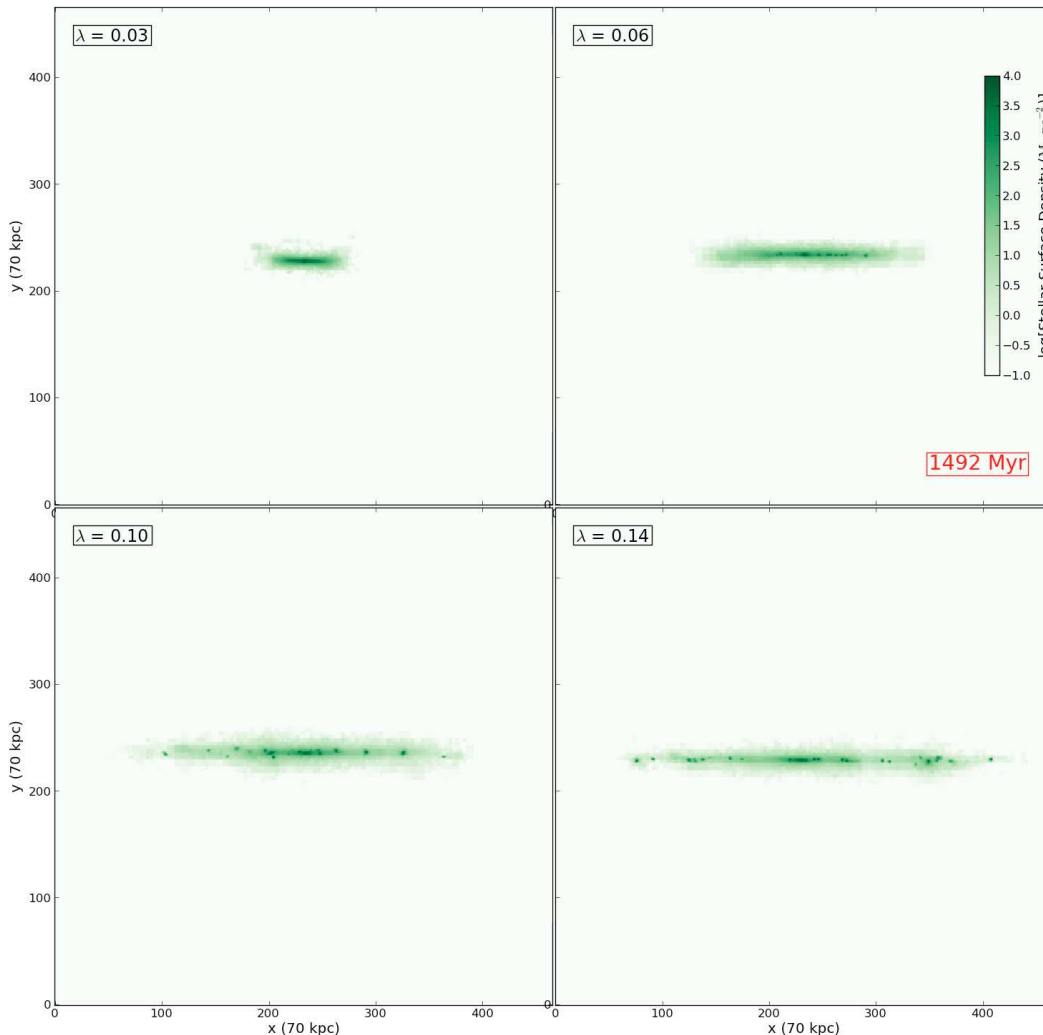


FIG. 2.— Same as Figure 1 but from the edge-on angle. $\lambda = 0.03, 0.06, 0.10, 0.14$ in the top-left, top-right, bottom-left, and bottom-right panel, respectively.

properties including surface brightnesses by adopting the following prescriptions for galaxy evolution: (a) an isothermal spherical halo, (b) a model for gas infall rate that reproduces the observed properties of the Milky Way, (c) the Schmidt law for star formation (Schmidt 1959), and (d) the galactic chemical evolution model by Matteucci & Francois (1989). They found nice agreement between the resulting predictions and the observed properties of LSBs such as surface brightness, metallicity, and colors, provided that the host halo satisfies the condition of $\lambda \geq 0.06$. This work was extended by Boissier et al. (2003) to a larger set of observational data and a wider range of halo spin parameters. They drew the same conclusion that a LSB is likely to form in a dark matter halo with a large spin parameter. They also noted that some modulation in the star formation rate history would be desired to achieve a better agreement between the theory and observations.

However, the conclusion reached by Jimenez et al. (1998) and Boissier et al. (2003) was contingent upon how the gas infall rate and star formation rate were prescribed in their overly simplified evolution models. It is still inconclusive whether the theoretical model by Dalcanton et al. (1997) would hold robustly in reality where the gas infall and star formation can hardly be specified by a simple analytic recipe. In what follows, we describe a suite of comprehensive, first-principles

numerical simulations of a galactic halo with realistic initial conditions, designed to better address this long-standing problem. Most importantly, unlike previous studies we do not rely on simplified prescriptions for star formation and gas infall rates, which for the first time enables us to examine the robustness of the theory in the most realistic set-up yet.

3. INITIAL CONDITIONS AND PHYSICS IN THE CODE

We simulate the evolution of a dwarf-sized galactic halo with varying halo spin parameters and initial baryon fractions. The initial conditions of our experiment and the physics included in the code are explained in this section.

We set up an isolated halo of total mass $2.3 \times 10^{11} M_{\odot}$ with four halo spin parameters, $\lambda = 0.03, 0.06, 0.10, 0.14$, and with two different initial baryon fractions for each λ , $f_b = (M_{\star} + M_{\text{gas}})/M_{\text{total}} = 0.05$ and 0.10 (see Table 1; 95% dark matter + 5% gas for $f_b = 0.05$, and 90% dark matter + 10% gas for $f_b = 0.10$). We first create a dataset of 10^6 collisionless particles, to which we add gas by splitting the particles (with an initial metallicity of $0.003 Z_{\odot}$). Gas and dark matter follow the same shapes of a Navarro-Frenk-White profile (Navarro et al. 1997) with concentration $c = 10$, and have the same value of λ as an averaged circular motion. This way, as the gas cools down, the progenitor forms a disk galaxy embedded in a gaseous halo. Note that this procedure is very dif-

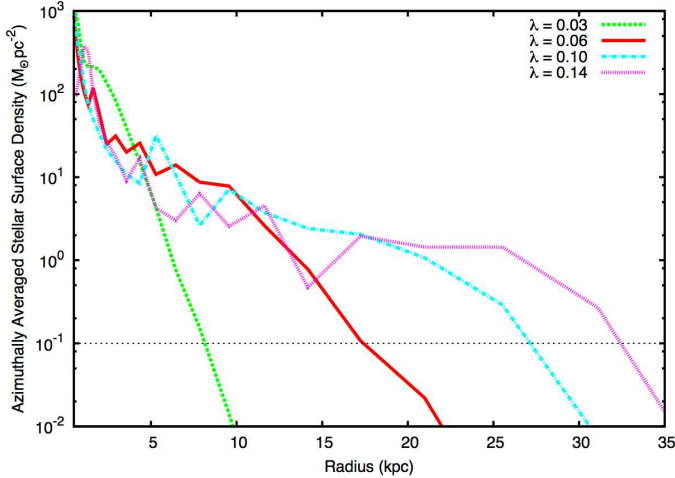


FIG. 3.— Azimuthally-averaged stellar surface densities at 1.49 Gyrs after the start of the simulation with $f_b = 0.10$ for $\lambda = 0.03, 0.06, 0.10, 0.14$ as a dashed, solid, dot-dashed, and dotted line, respectively. The scale radius r_s at which the stellar surface density falls below $0.1 M_\odot \text{pc}^{-2}$ monotonically increases as the halo spin parameter increases (see §4.1 and Table 1).

ferent from that of Jimenez et al. (1998) where a galactic disk already exists when their calculation starts. For detailed descriptions to set up the initial condition, see Kim et al. (2012).

We then follow the evolution of each galactic halo in a 1 Mpc^3 box for ~ 2 Gyrs using the ZEUS hydrodynamics solver included in the publicly available adaptive mesh refinement *Enzo-2.1.3*. Multi-species chemistry ($\text{H}, \text{H}^+, \text{He}, \text{He}^+, \text{He}^{++}, \text{e}^-$) and non-equilibrium cooling modules are employed to calculate radiative losses. Cooling by metals is estimated in gas above 10^4 K with the rates tabulated by Sutherland & Dopita (1993), and below 10^4 K by Glover & Jappsen (2007). We refine the cells by factors of two in each axis on the overdensities of gas and dark matter. In the finest cell of size $\Delta x = 122 \text{ pc}$, a star cluster particle is produced with initial mass $M_{\text{sc}}^{\text{init}} = 0.5 \rho_{\text{gas}} \Delta x^3$ when (a) the proton number density exceeds 3.2 cm^{-3} , (b) the velocity flow is converging, (c) the cooling time t_{cool} is shorter than the dynamical time t_{dyn} of the cell, and (d) the particle produced has at least $104000 M_\odot$. For each star cluster particle, 1.5×10^{-6} of its rest mass energy and 20% of its mass are returned to the gas phase over $12 t_{\text{dyn}}$. This represents various types of stellar feedback, chiefly the injection of thermal energy by supernova explosion. More information on adopted baryonic physics can be found in Kim et al. (2009) and Kim et al. (2011).

4. SIMULATION RESULTS

We now describe the results of our simulations with varying halo spin parameters and baryon fractions. First, we focus on the correlations between surface densities of a galactic disk and the spin parameter of its host halo in the simulations with an initial baryonic mass fraction of 10%.

4.1. Galactic Disks with Varying Spin Parameters

We start by calculating the stellar surface density of the simulated disk galaxy for each case of λ at 1.49 Gyrs after the start of the simulation with an initial baryon fraction $f_b = 0.10$, the ratio of baryonic mass to total mass. Shown in Figures 1 and 2 are the snapshots of face-on and edge-on

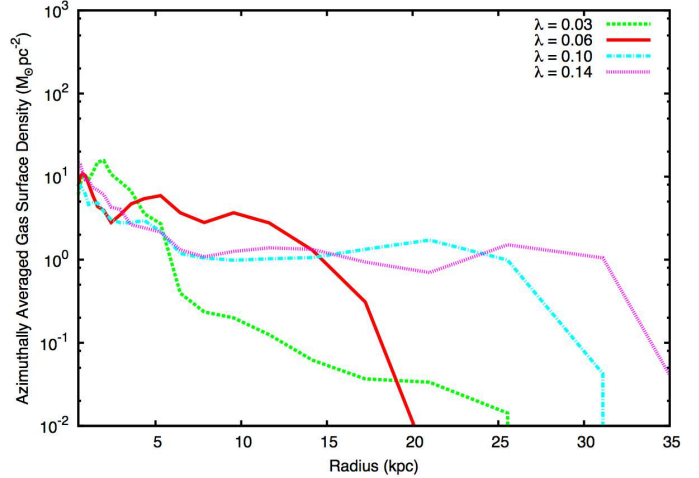


FIG. 4.— Same as Figure 4 but for azimuthally-averaged gas surface densities. The size of a gas disk increases with the halo spin parameter.

stellar surface densities using the stars of age less than 1 Gyr. In each figure, the four panels correspond to the four different values of halo spin parameters, $\lambda = 0.03, 0.06, 0.10, 0.14$. The snapshots are generated in a 70 kpc box with uniform 150 pc resolution which can be regarded as an equivalent of an aperture size in photometric observations. We also point out that, in these figures and the subsequent analysis, we exclude the stars formed in the first 0.49 Gyrs since they would most possibly reflect the artificial burst of star formation in the initially unimpeded collapse, caused by an unstable gas profile at the beginning of the simulation.⁴ From these figures, it is clearly noticeable that the size of the stellar disk is larger in the case of a higher value of λ , indicating that the large angular momentum of a dark matter halo disperses the baryonic content to a wider extent.

To quantify the change in the disk size resulting from different halo spin parameters, the radial profile of the stellar surface density, $\Sigma_*(r)$ (in the unit of $M_\odot \text{pc}^{-2}$), is determined by taking the azimuthal average of the stellar density on the disk plane at 1.49 Gyrs after the start of the simulation. The result of this exercise is displayed in Figure 3. Similarly, the radial profile of the azimuthally-averaged gas surface density, $\Sigma_{\text{gas}}(r)$, is shown in Figure 4. Then, the scale radius r_s is defined as the radius at which the stellar surface density drops below $0.1 M_\odot \text{pc}^{-2}$. Table 1 lists the scale radii for the four different λ , and the average stellar surface densities within those radii, $\Sigma_{*,\text{ave}}$. One can observe that the scale radius r_s monotonically increases as λ increases, from 8.1 kpc at $\lambda = 0.03$ to 32.5 kpc at $\lambda = 0.14$. The net effects are an enlarged photometric size of the stellar disk, and a lowered average stellar surface density $\Sigma_{*,\text{ave}}$: $278.2 M_\odot \text{pc}^{-2}$ at $\lambda = 0.03$ to $15.2 M_\odot \text{pc}^{-2}$ at $\lambda = 0.14$. As a result, the ratio of $\Sigma_{*,\text{ave}}$ for the case of $\lambda = 0.03$ to that of $\lambda = 0.14$ becomes larger than 15. This result confirms the idea that the faster rotation of the host halo disperses the disk gas to a larger extent, which then leads to a lower stellar surface density averaged on the disk. Assuming a plausible stellar mass-to-light ratio, the low stellar surface density is translated into the low surface

⁴ It should also be noted that we arbitrarily choose the epoch of 1.49 Gyrs for the analysis. Excluding the stars formed in the first 0.49 Gyrs we, therefore, implicitly assume that the stars younger than 1 Gyr form the disk of a dwarf-sized galaxy. While 1 Gyr may correspond to an interval between major disturbances for dwarf-sized galaxies, our choice is certainly very fiducial.

³ <http://enzo-project.org/>

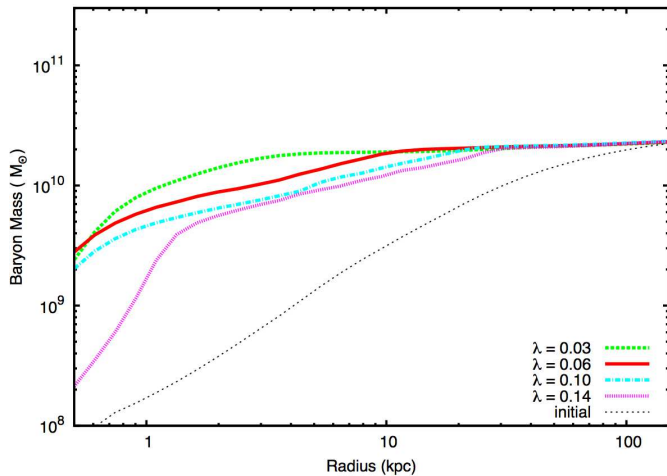


FIG. 5.— Radial profiles of enclosed baryonic mass (stars+gas) at 1.49 Gyrs after the start of the simulation with $f_b = 0.10$ for $\lambda = 0.03, 0.06, 0.10, 0.14$ as a thick dashed, solid, dot-dashed, and dotted line, respectively. The initial radial profile is also shown for comparison as a thin dotted line. While all the halos show the results of dissipative collapses towards the center, the halo of $\lambda = 0.03$ has the densest core in the baryon distribution.

brightness, giving consistent results with the previous studies by Jimenez et al. (1998) and Boissier et al. (2003).

It is also very informative to investigate how the mass profiles are correlated with the halo spin parameter. We evaluate the profiles of baryonic mass enclosed within a sphere of radius r from the galactic center of mass at 1.49 Gyrs after the start of the simulation. The resulting radial profiles in Figure 5 allow us to cleanly see the discrepancy across different runs in a cumulative manner. While all the halos show the results of dissipative collapses towards the center, the halo of the lowest spin parameter $\lambda = 0.03$ has the densest core in the baryonic distribution, enclosing most of the baryons within ~ 3 kpc from the center. We also inspect the half-mass radius that encloses a half of the total baryonic mass inside the halo, $\sim 2.2 \times 10^{10} M_\odot$. As is anticipated, the half-mass radius increases almost monotonically with λ , from 1.4 kpc at $\lambda = 0.03$ to 8.0 kpc at $\lambda = 0.14$. Finally Figure 6 demonstrates the profiles of the dark matter mass enclosed within a sphere of radius r . One can easily notice that the larger the halo spin parameter is, the less dense the dark matter distribution becomes in the core region ($r \lesssim 1$ kpc). In particular, the mass enclosed within a 1 kpc sphere in the $\lambda = 0.03$ case is $\sim 2.8 \times 10^9 M_\odot$, whereas that of $\lambda = 0.14$ case is only $\sim 6.0 \times 10^8 M_\odot$. This implies that dark matter itself is also gradually dispersed outwards by the fast rotation of the halo.

4.2. Robustness Against Variations in the Baryon Fraction

Now that we have found a strong correlation between the halo spin parameter and the stellar/gas surface densities of a galactic disk, it will be very illuminating to examine whether or not this correlation is robust against variations in the initial baryonic mass fraction f_b . This examination may also allow us to determine which factor is more dominant in determining the scale radius and galactic surface density, between the absolute amount of gas and the angular momentum of the host halo. Recall that the results presented in §4.1 are all obtained by the simulations with $f_b = 0.10$.

We here repeat the same analysis in Figure 3 but on a suite of simulations with a different initial baryon fraction, $f_b = 0.05$, and plot the result in Figure 7. First, as is obviously expected, a decreased value of f_b also reduces the

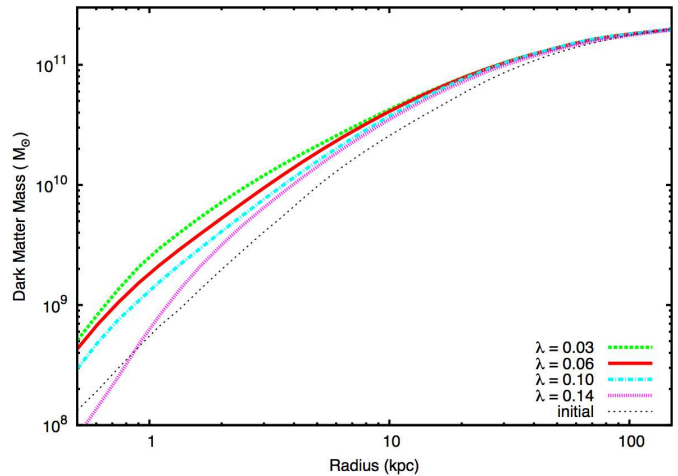


FIG. 6.— Same as Figure 5 but of the enclosed dark matter mass. Note that the halo of $\lambda = 0.03$ exhibits the most centrally-concentrated density profile.

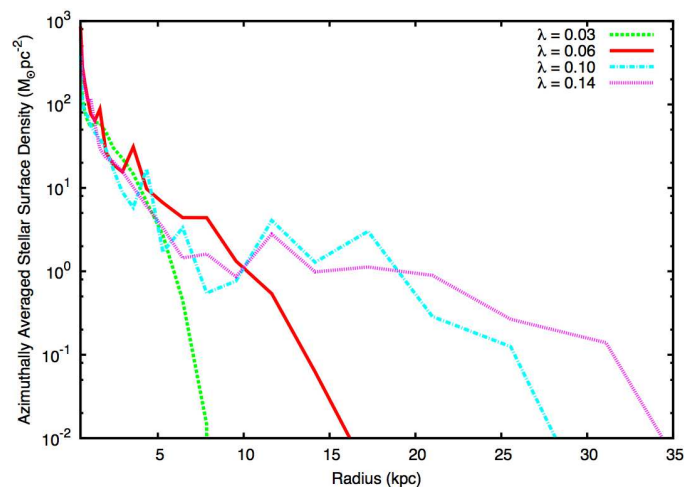


FIG. 7.— Same as Figure 3 but for the case of the initial baryonic mass fraction $f_b = 0.05$ instead of $f_b = 0.10$. The trend of an increasing scale radius with a larger halo spin parameter persists.

overall stellar surface density for a halo with the same spin parameter. What is more intriguing is that the positive correlation between the scale radius r_s (see §4.1) and the halo spin parameter λ still holds strong in simulations with a lower f_b : a faster rotation of the host halo induces a larger scale radius of the stellar disk. Table 1 lists the scale radii and the average stellar surface densities of the galactic disks within those radii for $f_b = 0.05$, which clearly shows that the correlations between r_s and λ holds the same for both f_b 's. Interestingly, the difference between two r_s 's for $f_b = 0.05$ and 0.10 with the same λ is surprisingly small. For example, the scale radius of a disk in the halo of $\lambda = 0.10$ and $f_b = 0.10$ is 26.8 kpc, only slightly expanded from 26.0 kpc in the halo of the same λ but of $f_b = 0.05$. This is despite the fact that the initial gas supply is boosted by a factor of two. Although it should be considered provisional this result may suggest that, between λ and f_b , the more influential factor for determining the scale radius is λ , the spin parameter of the halo.

4.3. Notes on the Performed Runs

Before we proceed to conclude, it is worth to note a few points on the simulations we have described so far. We draw

TABLE 1
HALO SPIN PARAMETER, DISK SCALE RADIUS, AND AVERAGE STELLAR SURFACE DENSITY^a

halo spin parameter λ	$f_b = 0.05$		$f_b = 0.10$	
	scale radius r_s [kpc]	$\Sigma_{*,\text{ave}}$ [$M_\odot \text{pc}^{-2}$]	scale radius r_s [kpc]	$\Sigma_{*,\text{ave}}$ [$M_\odot \text{pc}^{-2}$]
0.03	7.2	157.0	8.1	278.2
0.06	13.3	49.1	17.3	60.2
0.10	26.0	11.7	26.8	24.6
0.14	32.2	6.5	32.5	15.2

^aFor definitions and detailed explanation, see §4.1.

the reader’s attention to the central maximum stellar surface densities of the simulated galaxies in Figure 3, which still remain above or very close to $100 M_\odot \text{pc}^{-2}$ regardless of λ . Therefore, at face value, even the largest halo spin parameter seemingly fails to produce a LSB galaxy in its conventional definition (see §1). *However*, these simulations are under a particular assumption of a relatively high baryon fraction of $f_b = 0.10$. By comparing Figures 3 and 7, one observes that the central peak stellar surface density indeed drops significantly when the initial gas supply is reduced by a factor of two. Had the galaxy been simulated in a fast-rotating halo (e.g. $\lambda > 0.10$) with an even smaller baryon fraction (e.g. $f_b < 0.02$), it would likely have developed into a LSB galaxy with a central maximum stellar surface density less than $100 M_\odot \text{pc}^{-2}$. Further, by running simulations in an isolated set-up, we also have made an implicit assumption that the halo does not experience any interaction with its surrounding environment, such as mergers and harassment. Including such effects might have drastically changed the surface densities of the simulated galaxies.

In summary, the reported simulations are aimed to make a comparison between the galaxies that differ only by their halo spin parameters. Our experiment is however *not* specifically designed to turn *any* galaxy into a LSB with a large halo spin parameter. In reality, the galactic surface brightness is most likely determined by the combination of a number of factors such as halo angular momentum, baryon fraction, and environmental effects (see §5).

5. DISCUSSION AND CONCLUSION

We have presented the first numerical evidence for the hypothesis that late-type LSBs form in the halos with large angular momenta. A suite of comprehensive hydrodynamic simulations of a $2.3 \times 10^{11} M_\odot$ galactic halo is employed with different halo spin parameters and baryon fractions. We have investigated the correlations between the stellar/gas surface

densities of a galactic disk and the spin parameter of its host halo. A clear signal of anti-correlation is found between the surface densities and the halo spin parameter. That is, as the halo spin parameter increases, the scale radius, defined as the radius at which the stellar surface density drops below $0.1 M_\odot \text{pc}^{-2}$, monotonically increases, while the average stellar surface density of the disk within that radius decreases. The ratio of the average stellar surface density for the case of $\lambda = 0.03$ to that for the case of $\lambda = 0.14$ is larger than 15. Even dark matter itself is dispersed outwards by a large halo angular momentum. We also have demonstrated that the result is robust against variations in the initial value of the baryonic mass fraction.

Our investigation confirms that one of the most important drivers for the formation of LSBs is the spin parameters of their host halos. This work provides a critical link between observations and the theoretical models for the origin of LSBs, which has long been missing in the previous studies. It also enables us to better comprehend the formation process of LSBs, and to utilize LSBs for the purpose of constraining the nature of invisible component that dominates galactic dynamics. Even so, the reported calculation alone cannot decide whether the halo angular momentum is the most determinative factor in the formation of LSBs. There is a large multi-dimensional parameter space to explore, including the halo angular momentum, halo density profile, baryon fraction, gas infall rate, and stellar feedback, to name a few.

J. K. thanks Mark Krumholz for providing insightful comments and advice on the early version of this article. J. K. gratefully acknowledges support from the NSF Grant AST-0955300. J. L. acknowledges the financial support from the National Research Foundation of Korea (NRF) grant funded by the Korea government (MEST, No.2012-0004916) and from the National Research Foundation of Korea to the Center for Galaxy Evolution Research.

REFERENCES

- Bell, E. F., Barnaby, D., Bower, R. G., et al. 2000, MNRAS, 312, 470
 Bergmann, M. P., Jørgensen, I., & Hill, G. J. 2003, AJ, 125, 116
 Bergvall, N., Zackrisson, E., & Caldwell, B. 2010, MNRAS, 405, 2697
 Boissier, S., Monnier-Ragaine, D., Prantzos, N., et al. 2003, MNRAS, 343, 653
 Boissier, S., Gil de Paz, A., Boselli, A., et al. 2008, ApJ, 681, 244
 Bullock, J. S., Dekel, A., Kolatt, T. S., et al. 2001, ApJ, 555, 240
 Ceccarelli, L., Herrera-Camus, R., Lambas, D. G., Galaz, G., & Padilla, N. D. 2012, MNRAS, L500
 Dalcanton, J. J., Spergel, D. N., & Summers, F. J. 1997, ApJ, 482, 659
 de Blok, W. J. G., McGaugh, S. S., & van der Hulst, J. M. 1996, MNRAS, 283, 18
 de Blok, W. J. G., & McGaugh, S. S. 1997, MNRAS, 290, 533
 de Blok, W. J. G., & McGaugh, S. S. 1998, ApJ, 508, 132
 Doroshkevich, A. G. 1970, Astrofizika, 6, 581
 Fall, S. M., & Efstathiou, G. 1980, MNRAS, 193, 189
 Freeman, K. C. 1970, ApJ, 160, 811
 Galaz, G., Herrera-Camus, R., Garcia-Lambas, D., & Padilla, N. 2011, ApJ, 728, 74
 Gao, D., Liang, Y.-C., Liu, S.-F., et al. 2010, Research in Astronomy and Astrophysics, 10, 1223
 Gerritsen, J. P. E., & de Blok, W. J. G. 1999, A&A, 342, 655
 Glover, S. C. O., & Jappsen, A. 2007, ApJ, 666, 1
 Impey, C., Bothun, G., & Malin, D. 1988, ApJ, 330, 634
 Impey, C., & Bothun, G. 1997, ARA&A, 35, 267
 Irwin, M. J., Davies, J. I., Disney, M. J., & Phillipps, S. 1990, MNRAS, 245, 289
 Jimenez, R., Heavens, A. F., Hawkins, M. R. S., & Padoan, P. 1997, MNRAS, 292, L5
 Jimenez, R., Padoan, P., Matteucci, F., & Heavens, A. F. 1998, MNRAS, 299, 123
 Kim, J.-H., Wise, J. H., & Abel, T. 2009, ApJ, 694, L123
 Kim, J.-H., Wise, J. H., Alvarez, M. A., & Abel, T. 2011, ApJ, 738, 54
 Kim, J.-H., Krumholz, M. R., Wise, J. H., Turk, M. J., Goldbaum, N. J., & Abel, T. 2012, arXiv:1210.3361

- Kuzio de Naray, R., McGaugh, S. S., & de Blok, W. J. G. 2004, MNRAS, 355, 887
- Kuzio de Naray, R., & Spekkens, K. 2011, ApJ, 741, L29
- Lee, J., Zhao, G.-B., Li, B., & Koyama, K. 2012, arXiv:1204.6608
- Matteucci, F., & Francois, P. 1989, MNRAS, 239, 885
- Matthews, L. D., Gao, Y., Uson, J. M., & Combes, F. 2005, AJ, 129, 1849
- Matthews, L. D., & Wood, K. 2001, ApJ, 548, 150
- McGaugh, S. S., & Bothun, G. D. 1994, AJ, 107, 530
- McGaugh, S. S., Schombert, J. M., & Bothun, G. D. 1995, AJ, 109, 2019
- McGaugh, S. S., & de Blok, W. J. G. 1998, ApJ, 499, 41
- McGaugh, S. S., & de Blok, W. J. G. 1998, ApJ, 499, 66
- McGaugh, S. S., Rubin, V. C., & de Blok, W. J. G. 2001, AJ, 122, 2381
- Mihos, C., McGaugh, S., & de Blok, E. 1996, arXiv:astro-ph/9612115
- Mo, H. J., McGaugh, S. S., & Bothun, G. D. 1994, MNRAS, 267, 129
- Mo, H. J., Mao, S., & White, S. D. M. 1998, MNRAS, 295, 319
- Morelli, L., Corsini, E. M., Pizzella, A., et al. 2012, MNRAS, 423, 962
- Navarro, J. F., Frenk, C. S., & White, S. D. M. 1997, ApJ, 490, 493
- Peebles, P. J. E. 1969, ApJ, 155, 39
- Pickering, T. E., Impey, C. D., van Gorkom, J. H., & Bothun, G. D. 1997, AJ, 114, 1858
- Pizzella, A., Corsini, E. M., Sarzi, M., et al. 2008, MNRAS, 387, 1099 3
- Rosenbaum, S. D., Krusch, E., Bomans, D. J., & Dettmar, R.-J. 2009, A&A, 504, 807
- Schmidt, M. 1959, ApJ, 129, 243
- Schombert, J. M., & Bothun, G. D. 1988, AJ, 95, 1389
- Schombert, J. M., Bothun, G. D., Schneider, S. E., & McGaugh, S. S. 1992, AJ, 103, 1107
- Spergel, D. N., & Steinhardt, P. J. 2000, Physical Review Letters, 84, 3760
- Sprayberry, D., Impey, C. D., & Irwin, M. J. 1996, ApJ, 463, 535
- Sprayberry, D., Impey, C. D., Irwin, M. J., & Bothun, G. D. 1997, ApJ, 482, 104
- Steinmetz, M., & Bartelmann, M. 1995, MNRAS, 272, 570
- Sutherland, R. S., & Dopita, M. A. 1993, ApJS, 88, 253
- Swaters, R. A., Sanders, R. H., & McGaugh, S. S. 2010, ApJ, 718, 380
- Walker, M. G., McGaugh, S. S., Mateo, M., Olszewski, E. W., & Kuzio de Naray, R. 2010, ApJ, 717, L87
- White, S. D. M. 1984, ApJ, 286, 38
- Zhong, G. H., Liang, Y. C., Liu, F. S., et al. 2012, arXiv:1205.2404
- Zwaan, M. A., van der Hulst, J. M., de Blok, W. J. G., & McGaugh, S. S. 1995, MNRAS, 273, L35